Acta Cryst. (1995). D**51**, 605–608

Crystallization and Preliminary Structure of Porcine Aldehyde Reductase–NADPH Binary Complex

BY OSSAMA EL-KABBANI* AND KEN JUDGE

The University of Alabama at Birmingham, Center for Macromolecular Crystallography, Birmingham, Alabama 35294-0005, USA

STEPHAN L. GINELL

Argonne National Laboratory Structural Biology Center, c/o Brookhaven National Laboratory, Building 725, National Synchrotron Light Source, Beamline X8C, Upton, New York 11973-5000, USA

LAWRENCE J. DELUCAS

The University of Alabama at Birmingham, Center for Macromolecular Crystallography, Birmingham, Alabama 35294-0005, USA

AND T. GEOFFREY FLYNN

Queen's University, Department of Biochemistry, Kingston, Ontario K7L 3N6, Canada

(*Received* 14 *July* 1994; *accepted* 30 *November* 1994)

Abstract

Porcine aldehyde reductase–NADPH binary complex has been crystallized from a buffered ammonium sulfate solution. The crystal form is hexagonal, space group $P6_522$, with $a = b = 67.2$, $c = 243.7$ Å, $\alpha = \beta = 90.0$ and $\gamma = 120.0°$. A molecular-replacement structure solution has been successfully obtained by using the refined structure of the apoenzyme as the search model. The crystallographic R factor is currently equal to 0.24 after energy minimization using data between 8 and 3.0 Å resolution. The aldehyde reductase–NADPH complex model is supported by electron density corresponding to NADPH not included in the search model. The tertiary structure of aldehyde reductase consists of a β/α-barrel with the coenzyme-binding site located at the carboxy-terminal end of the strands of the barrel. The structure of aldehyde reductase–NADPH binary complex will help clarify the mechanism of action for this enzyme and will lead to the development of pharmacologic agents to delay or prevent diabetic complications.

Introduction

Aldehyde reductase (ALR1; E.C. 1.1.1.2) and aldose reductase (ALR2; E.C. 1.1.1.21) are members of the aldo-keto reductase superfamily which catalyzes the NADPH-dependent reduction of a variety of aliphatic and aromatic aldehydes such as sugars to their corresponding alcohols (Flynn, 1982). The physiological role for these two enzymes has not yet been identified. However, their ability to reduce the excess glucose that results from the hyperglycemia of diabetes mellitus to sorbitol has been linked to diabetic complications affecting the eyes, kidneys and nervous system (Kinoshita & Nishimura, 1988). Side effects and/or lack of efficacy have prevented several excellent inhibitors of aldose and aldehyde reductase from achieving approval for clinical use (Srivastava, Petrash, Sanada, Ansari & Patridge, 1982; Spielberg, Shear, Cannon, Hutson & Gunderson, 1991). In order to develop potent and more specific inhibitors for aldose and aldehyde reductase, attention has been turned to the possibilities of drug design based on the three-dimensional structures of these two enzymes and their mechanisms of action.

The structure of porcine aldose reductase complexed with the coenzyme analog 2′-monophosphoadenosine-5′-diphosphoribose (ADPRP) has been reported (Rondeau *et al.*, 1992), as has the structure of the ternary complex of human aldose reductase with coenzyme and the potent active-site inhibitor zopolrestat (Wilson, Tarle, Petrash & Quiocho, 1993). In addition, the mechanism of action for aldose reductase has been described (Wilson, Bohren, Gabbay & Quiocho, 1992; Harrison, Bohren, Ringe, Petsko & Gabbay, 1994). Aldehyde reductase apoenzyme from porcine and human kidneys was crystallized from buffered ammonium sulfate solutions. We have determined the three-dimensional structures of porcine and human aldehyde reductase by using a combination of molecular-replacement and isomorphous-replacement techniques (El-Kabbani *et al.*, 1993, 1994).

To assist in the refinement of the crystal structure of the enzyme, the cDNA of pig brain aldehyde reductase

* Author to whom correspondence should be addressed.

was cloned and the amino-acid sequence determined (Green, El-Kabbani & Flynn, 1994). The remarkable homology (97%) that exists between the primary structures of porcine aldehyde reductase and human aldehyde reductase is also reflected in their tertiary structures. The tertiary structures of aldehyde reductase and aldose reductase are similar and consist of an eight-stranded β/α-barrel or triose phosphate isomerase barrel (TIM-barrel) with the coenzyme-binding site located at the carboxy-terminal end of the strands of the barrel. In addition, two short antiparallel β-strands at the N-terminus, three large exposed loops and two α-helices are observed in both the aldose and aldehyde reductase molecules.

Since the three-dimensional structure of aldehyde reductase was determined without a bound ligand, it is difficult to predict the exact interactions of aldehyde reductase with cofactor and substrate. In order to clarify the mechanism of action of aldehyde reductase, it will be important to determine the structure of the enzyme complexed with cofactor and a substrate analog. In addition, this level of structural information will allow the design of new inhibitors which will be more specific and potent than those presently available, since many of the current inhibitors appear to bind to the enzyme–NADPH complex.

Experimental

Purification, crystallization and data collection

Porcine kidney aldehyde reductase was isolated and purified using a modification of the method of Cromlish & Flynn (1983). The two modifications to the published method were: (1) use of a Tris buffer system instead of sodium phosphate. (2) Inclusion of size-exclusion high-performance liquid chromatography as the final purification step. Hexagonal crystals of porcine aldehyde reductase–NADPH binary complex were grown at 295 K by vapor diffusion using the hanging-drop method (McPherson, 1985). Stock solutions were made by taking 60 µl protein (18 mg ml^{-1}) previously dialyzed against 5 m*M* 2-mercaptoethanol, pH 6.2–6.5, and mixing with 25 µl of 49 m*M* NADPH. Each droplet consisted of 1 µl of protein–NADPH mixture, mixed with 1 µl of 2.4 *M* ammonium sulfate, 0.1 *M* citrate buffer, pH 4.0–5.0, equilibrated by vapor diffusion against a well solution of 1 ml of 2.4 *M* ammonium sulfate, 0.1 *M* citrate buffer, pH 4.0–5.0. Crystals grew to their maximum dimensions within 2–3 weeks (Fig. 1).

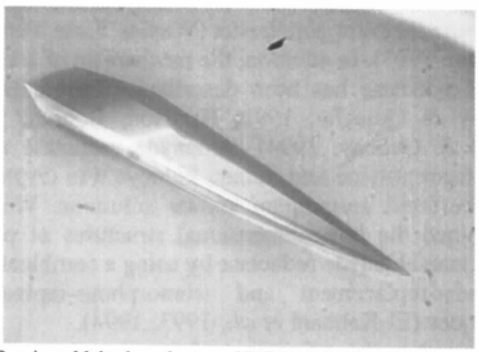

Fig. 1. Porcine aldehyde reductase–NADPH binary complex hexagonal crystal. Crystal dimensions: 0.45 × 0.15 × 0.15 mm.

Table 1. *Variation of $I/\sigma(I)$ with resolution*

$I/\sigma(I)$	0–3	3–6	6–9	9–12	12–15
No. of unique reflections 0–4.2 Å	453	365	264	227	1096
No. of unique reflections 4.2–3.0 Å	1087	724	358	234	380

Diffraction data were collected from one aldehyde reductase/NADPH complex crystal at 277 K using a CCD electronic area detector at the Argonne National Laboratory beamline X8C at the National Synchrotron Light Source, Brookhaven National Laboratory. Data frames were collected for 40 s using 0.2° ω-scans at a crystal-to-detector distance of 280 mm and a wavelength of 1.03 Å. The crystal form is hexagonal, space group $P6_522$ with $a = b = 67.2$, $c = 243.7$ Å, $\alpha = \beta = 90.0°$ and $\gamma = 120.0°$. The value for V_m is 2.24 Å Da^{-1} for a solvent content of 45%, and one molecule per asymmetric unit. Diffraction data were collected from one crystal (0.1 × 0.1 × 0.25 mm) to 2.9 Å resolution and processed using the *MADNES* program package (Messerschmidt & Pflugrath, 1987). The total number of observed reflections was 10 639 and the final data set had 5188 out of 6190 possible unique reflections at 3.0 Å resolution with an overall $R_{\rm merge}$ of 0.15. The variation of $I/\sigma(I)$ with resolution is shown in Table 1.

Recently, we have successfully optimized the crystallization conditions and obtained crystals of aldehyde reductase–NADPH binary complex that diffract to higher resolution. The modification to the crystallization conditions described above was using a mixture of 2.0 *M* ammonium sulfate, 0.1 *M* Tris buffer, pH 8.5 instead of 2.4 *M* ammonium sulfate, 0.1 *M* citrate buffer, pH 4.0–5.0. The new crystals are isomorphous with the crystals described above and diffract to 2.1 Å resolution at the Synchroton Radiation Source at Daresbury Laboratory (Fig. 2). High-resolution synchrotron data collection is currently in progress.

Results and discussion

Molecular-replacement studies

A rotation-translation function solution has been obtained using the 2.8 Å refined porcine aldehyde reductase apoenzyme structure (El-Kabbani *et al.*, 1994) as the search model. The crystal form of the apoenzyme is monoclinic, space group $P2_1$, with $a = 56.2, b = 98.1, c = 73.2$ Å, $\beta = 112.5°$. Rotation and translation searches were carried out using the *X-PLOR* program package (Brünger, Krukowski & Erickson, 1990). The Euler angles defining the highest rotation peak ($\theta1 = 189.6$, $\theta2 = 32.5$ and $\theta3 = 149.6°$) in the rotation search, using the 2408 reflections between 15

and 4 Å resolution with $F > 3\sigma(F)$, were applied directly to the model without any Patterson correlation refinement. Translation search using amplitudes between 8 and 3.5 Å resolution displayed one peak of 8.9 standard deviations above background. The translation distances in fractional coordinates in the x, y and z directions for the molecule calculated from its initial position equaled 0.040, 0.778 and 0.040, respectively. The crystallographic R factor for the molecular replacement solution equaled 0.38 using the 2958 reflections from 8 to 3.5 Å resolution with $F > 3\sigma(F)$.

Rigid-body refinement followed by 40 energy minimization steps (Brünger *et al.*, 1990) decreased the R factor to 0.33 and 0.24, respectively, using the 3910 reflections between 8 and 3 Å resolution with $F > 3\sigma(F)$ (90% of the observed unique reflections). The root-mean-square (r.m.s.) deviation of bond lengths and bond angles from ideality equaled 0.022 Å and 2.4°, respectively. Amino-acid side chains of the search model were fitted into a $(2F_o - F_c)$ electron-density map. The cofactor NADPH-binding site was located from a difference electron-density map calculated with coefficients $(F_o - F_c)$ and α_c at 3.0 Å resolution (Fig. 3). The NADPH-binding site of aldehyde reductase is located at the carboxy-terminal end of the strands of the β-barrel. Similar to aldose reductase (Wilson *et al.*, 1992), NADPH is bound to aldehyde reductase in an extended conformation and held in place by loop B (residues, 213–230) and a number of hydrogen bonds, salt links and van der Waals contacts from the strands of the β-barrel (Fig. 4).

At the present stage of refinement, the critical NADPH-binding residues for aldose reductase are conserved in aldehyde reductase and play a critical role in the NADPH-binding site for this enzyme. Moreover, these residues adopt similar conformations in the tertiary structures of human and porcine aldehyde reductase apoenzymes with r.m.s. differences of 0.35 and 0.94 Å between main-chain atoms and all atoms, respectively (El-Kabbani *et al.*, 1994). On the other hand, Wilson *et al.* (1992) predict that the substrate-binding site may exist in a region with fewer conserved residues compared to the residues forming the cofactor-binding site which may be responsible for differences in substrate specificities between aldose and aldehyde reductase.

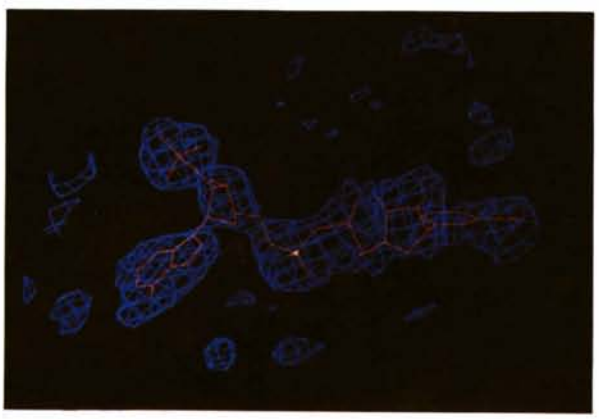

Fig. 3. NADPH (red) with superimposed difference electron density (blue) contoured at 2σ. The density was calculated after energy minimization with NADPH excluded from the model using coefficients $(F_o - F_c)$ and α_c at 3.0 Å resolution.

Fig. 4. Superposition of human aldose reductase (silver) and porcine aldehyde reductase (gold) with bound NADPH. The root-mean-square (r.m.s.) difference between main-chain atoms for human aldose reductase and porcine aldehyde reductase is 1.4 Å. Atomic coordinates for human aldose reductase (Wilson *et al.*, 1992) were obtained from the Protein Data Bank. NADPH is color coded according to atom type (O atoms are red, C atoms are green, N atoms are blue and P atoms are magenta). Ribbon drawings were prepared by using the programs described by Carson (1987).

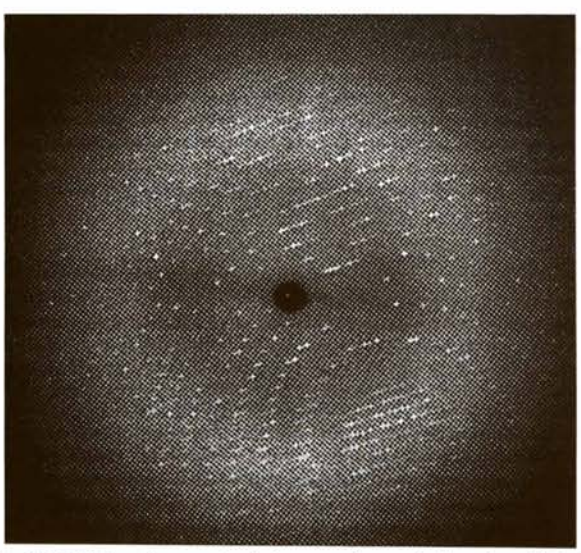

Fig. 2. Ocillation photograph of a hexagonal crystal of porcine aldehyde reductase–NADPH binary complex, taken at the Synchrotron Radiation Source, Daresbury Laboratory. The edge of the diffraction pattern represents 2.1 Å data.

A space-filling model of the non-H atoms of the aldehyde reductase molecule and NADPH is shown in Fig. 5. A portion of the nicotinamide ring is seen in the center and the 5′-phosphate and part of the adenosine are to the left. The pyrophosphate bridge of NADPH is tied down by loop *B* which holds NADPH tightly in place (the positions of residues 218–226 from loop *B* were not located in the structure of the apoenzyme). A conformational change of loop *B* is necessary for the association and dissociation of NADPH. An estimated rotation by 51° of loop *B* around Gly214 and Ser215 upon binding of NADPH to aldose reductase has been reported (Borhani, Harter & Petrash, 1992).

It has been proposed (Wilson *et al.*, 1992) that the 4-*pro-R* H atom from the exposed C-4 of the nicotinamide of NADPH bound to aldose reductase is transferred to the C atom of the carbonyl group of the substrate, followed by the protonation of the substrate carbonyl O atom by one of the two most likely conserved candidates, Tyr48 or His110. The kinetic mechanism of aldehyde reductase is believed to be the same as that of aldose reductase although the rate-determining step of this enzyme has not actually been defined. However, on the assumption that the catalytic mechanism of aldehyde reductase will be the same or very similar to that of aldose reductase, the activity of recombinant enzyme where the histidine and tyrosine residues have been mutated will be examined and the crystal structures determined.

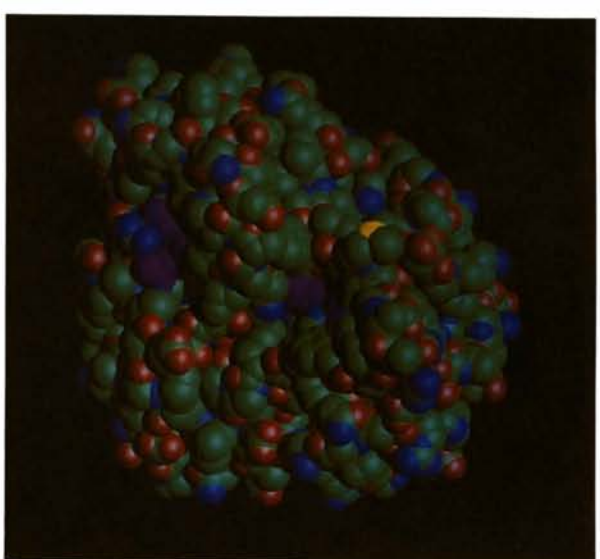

Fig. 5. Space-filling model of the non-H atoms of the porcine aldehyde reductase molecule with bound NADPH (magenta). The porcine aldehyde reductase molecule is color coded according to atom type (O atoms are red, C atoms are green, N atoms are blue and S atoms are yellow).

Attempts are currently under way to cocrystallize aldehyde reductase complexed with cofactor and various inhibitors. By studying the interactions of these compounds with the aldehyde reductase molecule, detailed knowledge regarding the chemical interactions will be made available. This structural information should allow the design of more effective compounds, perhaps active-site inhibitors that are more specific and have fewer side effects which could be used to alleviate some of the degenerative problems associated with diabetes.

We thank Dr Craig Smith for his assistance with synchrotron data collection. This work was supported by a research grant from the American Diabetes Association (to OEl-K) and from the Medical Research Council of Canada (to TGF). The Argonne National Laboratory Structural Biology Center at beamline X8C of the National Synchrotron Light source is supported by the United States Department of Energy, Office of Health and Environmental Research. The authors thank Maxine Rice for preparation of the manuscript.

References

Borhani, D. W., Harter, T. M. & Petrash, J. M. (1992). *J. Biol. Chem.* **267**, 24841–24847.

Brünger, A. T., Krukowski, A. & Erickson, J. (1990). *Acta Cryst.* A**46**, 585–593.

Carson, M. (1987). *J. Mol. Graphics*, **5**, 103–106.

Cromlish, J. A. & Flynn, T. G. (1983). *J. Biol. Chem.* **258**, 3583–3586.

El-Kabbani, O., Green, N. C., Lin, G., Carson, M., Narayana, S. V. L., Moore, K. M., Flynn, T. G. & DeLucas, L. J. (1994). *Acta Cryst.* D**50**, 859–868.

El-Kabbani, O., Lin, G., Narayana, S. V. L., Moore, K. M., Green, N. C., Flynn, T. G. & DeLucas, L. J. (1993). *Acta Cryst.* D**49**, 490–496.

Flynn, T. G. (1982). *Biochem. Pharmacol.* **31**, 2705–2712.

Green, N. C., El-Kabbani, O. & Flynn, T. G. (1994). *FASEB J.* **8**. Abstract 217.

Harrison, D. H., Bohren, K. M., Ringe, D., Petsko, G. A. & Gabbay, K. H. (1994). *Biochemistry*, **33**, 2011–2020.

Kinoshita, J. H. & Nishimura, C. (1988). *Diabetes Metab. Rev.* **4**, 323–337.

McPherson, A. (1985). *Methods Enzymol.* **114**, 112–120.

Messerschmidt, A. & Pflugrath, J. W. (1987). *J. Appl. Cryst.* **20**, 306–315.

Rondeau, J.-M., Tête-Favier, F., Podjarny, A., Reymann, J.-M., Barth, P., Biellmann, J. F. & Moras, D. (1992). *Nature (London)*, **355**, 469–472.

Spielberg, S. P., Shear, N. H., Cannon, M., Hutson, N. J. & Gunderson, K. (1991). *Ann. Int. Med.* **114**, 720–724.

Srivastava, S. K., Petrash, J. M., Sanada, I. J., Ansari, N. H. & Patridge, C. A. (1982). *Curr. Eye Res.* **2**, 407–410.

Wilson, D. K., Bohren, K. M., Gabbay, K. H. & Quiocho, F. A. (1992). *Science*, **257**, 81–84.

Wilson, D. K., Tarle, I., Petrash, J. M. & Quiocho, F. A. (1993). *Proc. Natl Acad. Sci. USA*, **90**, 9847–9851.